Contents lists available at ScienceDirect

Experimental Neurology

journal homepage: www.elsevier.com/locate/yexnr

Regular Article

Riluzole promotes motor and respiratory recovery associated with enhanced neuronal survival and function following high cervical spinal hemisection

CrossMark

K. Satkunendrarajah [a], F. Nassiri [a], S.K. Karadimas [b], A. Lip [a], G. Yao [a], M.G. Fehlings [a,b,*]

[a] Department of Genetics and Development, Toronto Western Research Institute, and Spinal Program, Krembil Neuroscience Center, University Health Network, Toronto, Ontario, Canada
[b] Department of Surgery, University of Toronto, Ontario, Canada

ABSTRACT

Cervical spinal cord injury (SCI) can result in devastating functional deficits that involve the respiratory and hand function. The mammalian spinal cord has limited ability to regenerate and restore meaningful functional recovery following SCI. Riluzole, 2-amino-6-trifluoromethoxybenzothiazole, an anti-glutamatergic drug has been shown to reduce excitotoxicity and confer neuroprotection at the site of injury following experimental SCI. Based on promising preclinical studies, riluzole is currently under Phase III clinical trial for the treatment of SCI (ClinicalTrials.gov: NCT01597518). Riluzole's anti-glutamatergic role has the potential to regulate neuronal function and provide neuroprotection and influence glutamatergic connections distal to the initial injury leading to enhanced functional recovery following SCI. In order to investigate this novel role of riluzole we used a high cervical hemisection model of SCI, which interrupts all descending input to motoneurons innervating the ipsilateral forelimb and diaphragm muscles. Following C2 spinal cord hemisection, animals were placed into one of two groups: one group received riluzole (8 mg/kg) 1 h after injury and every 12 h thereafter for 7 days at 6 mg/kg, while the second group of injured rats received vehicle solution for the same duration of time. A third group of sham injured rats underwent a C2 laminectomy without hemisection and served as uninjured control rats. Interestingly, this study reports a significant loss of motoneurons within the cervical spinal cord caudal to C2 hemisection injury. Disruption of descending input led to a decrease in glutamatergic synapses and motoneurons caudal to the injury while riluzole treatment significantly limited this decline. Functionally, Hoffmann reflex recordings revealed an increase in the excitability of the remaining ipsilateral cervical motoneurons and significant improvements in skilled and unskilled forelimb function and respiratory motor function in the riluzole-treated animals. In conclusion, using a C2 hemisection injury model, this study provides novel evidence of motoneuron loss caudal to the injury and supports riluzole's capacity to promote neuronal preservation and function of neural network caudal to the SCI resulting in early and sustained functional improvements.

© 2015 The Authors. Published by Elsevier Inc. This is an open access article under the CC BY-NC-ND license (http://creativecommons.org/licenses/by-nc-nd/4.0/).

1. Introduction

High cervical spinal cord injury (SCI) disrupts supraspinal connections to lower motoneurons and spinal circuitry leading to significant loss of sensory, motor and respiratory function. Majority of injuries to the spinal cord occur at the cervical level and are incomplete, with spared axonal connections to cervical respiratory and somatic motoneurons from supraspinal centers. The central nervous system shows limited capacity to regenerate following partial injuries (Kerschensteiner et al., 2004; Raineteau et al., 2002), however, spontaneous locomotor and respiratory recovery can occur to a limited extent associated with various forms of anatomical and functional plasticity within the caudal cervical region

(Lane et al., 2008). This spontaneous plasticity-mediated recovery in itself is not sufficient and leads to limited functional recovery and, as such, effective therapeutic strategies are needed to promote sensory, motor and autonomic functional recovery following SCI (Dougherty et al., 2012). Further, many strategies to strengthen connectivity have presumed that motoneurons within the cervical spinal cord remain intact after high cervical hemisection injury. The fate of motoneurons within the cervical neural circuitry distal to a left C2 hemisection injury is not known. Synergistic neural tissue protection and promotion of structural and functional plasticity of the spared circuitry caudal to the injury is a promising option for restoring meaningful functional recovery.

Loss of descending excitatory input to motoneurons caudal to the injury site leads to the paralysis of muscles innervated by these unexcitable motoneurons. Based on promising preclinical data, riluzole, the only FDA approved drug for ALS and a glutamatergic modulator, is currently in Phase III clinical trial for the treatment of SCI (Grossman

* Corresponding author at: Division of Neurosurgery, Toronto Western Hospital, 399 Bathurst St., Suite 4WW-449, Toronto, Ontario M5T2S8, Canada.
E-mail address: michael.fehlings@uhn.ca (M.G. Fehlings).

et al., 2014; Wilson and Fehlings, 2014). Using rodent models of SCI, riluzole has been demonstrated to increase tissue preservation at the site of injury leading to locomotor functional recovery (Wu et al., 2013; Schwartz and Fehlings, 2001). In the CNS, riluzole inhibits glutamate release and promotes reuptake by astrocytes resulting in improved glutamatergic regulation (Anon., 2003; Frizzo et al., 2004; Heurteaux et al., 1994; Kim et al., 2007; Kniest et al., 2001; Pereira et al., 2014). In addition, riluzole also has the ability to modulate synaptic activation of the ionotropic glutamate receptors N-methyl-D-aspartate (NMDA) and 2-amino-3-(3-hydroxy-5-methyl-isoxazol-4-yl) propanoic acid (AMPA). Both NMDA and AMPA receptor modulation of neurons play a key role in synaptic plasticity (Malinow and Malenka, 2002; Mantilla et al., 2012). At the acute stage, in the injured spinal cord, riluzole's role in decreasing intraspinal glutamate levels and excitotoxicity to promote tissue preservation has been demonstrated by our laboratory and others. Tissue preservation can be a significant mediator of functional recovery following SCI as it has been demonstrated that even a small amount of tissue preservation can lead to substantial functional recovery (Fehlings and Tator, 1995). However, riluzole's ability to modulate synaptic glutamate receptors to enhance synaptic strength, amplify motoneuron excitability and protect motoneurons caudal to the injury site has not been explored following SCI. Further examination and understanding of these mechanisms is important to optimize its use in the clinic.

Here, we interrogated the hypothesis that high cervical SCI mediated decrease in synaptic input onto caudal motoneurons leads to a decrease in their excitability and survival. Most importantly, for the first time this study reveals that a sharp hemisection injury to the cervical spinal cord at C2 leads to significant loss of motoneurons within a specified region of the cervical enlargement. Also, this study demonstrates that acute and subacute administration of riluzole following C2 hemisection partially restores respiratory related diaphragmatic function and promotes forelimb motor recovery by preventing this loss of motoneurons and enhancing their glutamate receptor-mediated connectivity.

2. Materials and methods

All experimental procedures were performed on male Wistar rats (2–3 months; 300–325 g; Jackson laboratories). Animal care and handling were conducted with the approval of the animal care committee of the University Health Network in accordance with the policies outlined in the guide on the care and use of experimental animals prepared by the Canadian Council of Animal Care. Rats were housed individually with free access to food and water.

2.1. Experimental design

40 rats were subjected to complete left hemisection of the spinal cord from the midline below the C2 dorsal roots. Injured animals were placed into one of two groups: one group of animals received intraperitoneal (IP) administration of riluzole (Sigma, R116) (8 mg/kg) 1 h post-C2 hemisection injury and every 12 h thereafter for 7 days at 6 mg/kg (n = 18). A second group of injured rats served as vehicle treated controls and were administered vehicle solution 1 h post-injury and twice daily (IP) for the same duration of time (n = 17). Riluzole was dissolved in 30% (w/v) of solubilizer 2-hydroxypropyl-β-cyclodextrin (HBC, Sigma, H-107). A third group of sham injured rats underwent a C2 laminectomy without hemisection and served as uninjured control rats (n = 5). An investigator blinded to the experimental groups prepared all experimental drugs and the dose of riluzole used in this study was based on our previous work on the pharmacodynamic and kinetic properties of riluzole (Wu et al., 2013). Spontaneous and riluzole-induced changes in skilled and unskilled forelimb function were monitored for 6 weeks post-injury. Terminal electrophysiological experiments were performed at 2 and 6 weeks to evaluate respiratory functional recovery and motoneuron excitability, respectively (Fig. 1).

2.2. Spinal cord injury: C2 hemisection

35 rats were anesthetized with 2% isoflurane in oxygen (1 l/min) and placed in a stereotaxic frame on a heating pad at 37 °C. Under aseptic conditions, following a midline dorsal incision the superficial muscles were retracted to expose the dorsal spinal cord. Following a C2 laminectomy and durotomy, the left side of the spinal cord was hemisected from the midline extending to the lateral spinal cord using microscissors (Kajana and Goshgarian, 2008). The hemisection was just caudal to the dorsal roots of the second cervical segment and the dorsal roots were not injured. A surgical probe was used to ensure anatomical completeness of the hemisection by scraping the floor and walls of the vertebral canal adjacent to the lesion. Following surgery, all animals received analgesic (Buprenorphine 0.5 mg/kg; twice daily for 48 h) and 10.0 ml of saline subcutaneously. Animals were placed under heat lamps in individual cages to recover during post-operative recovery period. The rats were maintained in a 12-h light/dark cycle in a temperature-controlled room at 27 °C for the duration of the experiment. Spinal tissue at the site of injury was stained with hematoxylin and eosin to confirm the completeness of the hemisection injury. In order to verify the loss of cervical motoneurons, a left C2 hemisection injury or sham surgery was performed in a group of ChAT-eGFP transgenic mice that express the green fluorescence protein (GFP) under the control of choline acetyltransferase promotor (Jackson Laboratory B6.Cg-Tg(RP23-268L19-EGFP)2Mik/J). This transgenic mouse line allows for fluorescent visualization of cholinergic motoneurons and cholinergic interneurons in the neonate as well as in adult mice. 6 weeks after the left C2 hemisection or sham surgery, the spinal cord from C2 to T3 was examined for expression of eGFP expressing neurons in the ventral horn.

2.3. Functional assessments

Investigators blinded to treatment groups carried out all of the neurobehavioral assessments and analysis from day one until 6 weeks post-injury.

2.4. Forelimb grip strength assessment

Ipsilateral and contralateral forelimb grip strengths were individually evaluated using a grip strength meter (Grip Strength System, DFM-1d; San Diego Instruments, San Diego, CA) every other day during the first 2 weeks (at days 1, 3, 5, 7, 9, 11, 13, and 15) and once per week during weeks 3, 4, 5 and 6. The animals were held parallel to a series of metal grip bars and allowed to grasp the bar individually with the ipsilateral alone and contralateral forelimb. After grasping the bar, animals were pulled away parallel to the degree they were held at until they released the bar and their grip force was measured. Ipsilateral and contralateral grip strengths were tested five times per session. The average ipsilateral and contralateral grip strength in grams of force was recorded for ipsilateral and contralateral forelimbs of each animal at each assessment.

2.5. Paw placement test

Spontaneous forelimb usage was evaluated during explorative behavior in a transparent cylinder of 20 cm in diameter and 30 cm in height at 2, 4 and 6 weeks after injury. A mirror placed behind the cylinder was used to observe forelimb movements from all angles. The use of the cylinder encouraged vertical exploration using the forelimb and the behavior was recorded and analyzed offline in slow motion. The number of times the animal reached up and placed its ipsilateral forelimb, contralateral forelimb or both forelimbs was recorded. Ipsilateral and contralateral forelimb placements were represented as the percentage of the total number of paw placements [% ipsilateral/contralateral forelimb placement = (ipsilateral/contralateral forelimb placement + both forelimb placement) / total forelimb placements × 100].
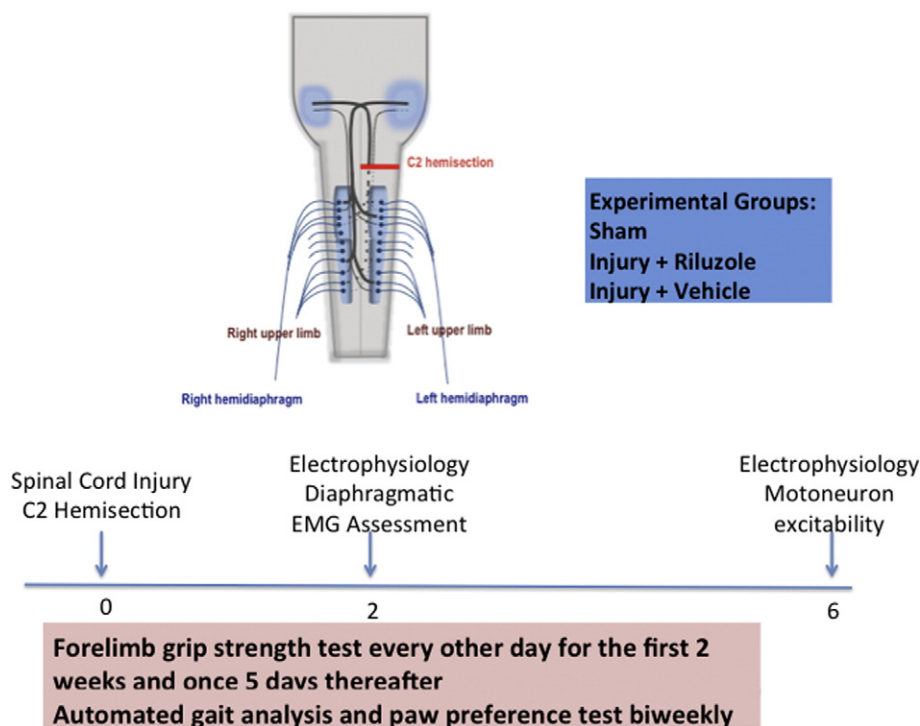
Fig. 1. Schematic view of the forelimb and respiratory circuitry in the cervical spinal cord and the experimental design.

2.6. CatWalk analysis

To further elucidate the forelimb and forepaw function across the experimental groups, gait analysis using the CatWalk gait analysis system was performed at 2 and 4 weeks post-injury for sham operated (n = 4), vehicle treated (n = 7) and riluzole treated (n = 7) animals as has been previously described (Karadimas et al., 2013; Iwasaki et al., 2014). In this study, following labeling of the digital prints collected via the CatWalk the following parameters were examined: a) paw print width (horizontal distance of the entire paw), b) paw print length (vertical distance of the entire paw), c) stride length, and d) swing speed for both ipsilateral and contralateral forelimbs.

2.7. Motoneuron excitability

Seven weeks post-C2 hemisection, terminal electrophysiological experiments were performed to assess cervical motoneuron excitability. Riluzole-treated (n = 6) and vehicle-treated (n = 6) injured rats as well a group of sham injured (n = 4) rats were subjected to frequency dependent depression of the H-reflex in ipsilateral and contralateral forelimbs. H-reflex recordings from both forelimbs were performed under isoflurane anesthesia. The ulnar nerves in the forelimbs were stimulated with bipolar needle electrodes and EMG activity was recorded from interosseus muscles of the forelimbs. H-response was stimulated with increasing intensities to determine the threshold to elicit the H-response and the maximum M- and H-wave responses. Subsequently, the intensity that elicited maximal H-response was used to deliver pulses at 0.2, 1, 2 and 5 Hz. The EMG activity was amplified and filtered between 10 and 3000 Hz. The maximal M and H wave amplitudes were measured and expressed as Hmax/Mmax ratio. Hmax/Mmax ratio, which represents motor neuron excitability, was calculated for each stimulation frequency.

2.8. Respiratory motoneuron output

Diaphragmatic EMG recording from the ipsilateral hemidiaphragm was used to determine the ability of riluzole to increase the efficacy of spared spinal connections to the cervical respiratory motoneurons in a subset of the injured animals. Two weeks post C2 hemisection injury, under isoflurane anesthesia a laparotomy was performed at the base of the rib cage to access the abdominal surface of the diaphragm. Bipolar silver electrodes were inserted bilaterally into the diaphragm and EMG muscle activity was differentially amplified at 10,000× and filtered (0.1–3 kHz) and acquired using a Cambridge Electronic Data acquisition system (CED1401) and Spike 2 software (Kajana and Goshgarian, 2008; Alilain and Goshgarian, 2008). To ensure standardized recording conditions, animals from all experimental groups were maintained on a heating pad. Qualitative analysis of the ipsilateral hemidiaphragmatic EMG recording was used to determine the number of animals that displayed respiratory related EMG activity on the ipsilateral hemidiaphragm. Subsequently, the recovered hemidiaphragmatic activity was rectified and integrated using the CED spike 2 data analysis software and 60 s of respiratory related activity was quantified. Mean integrated inspiratory burst area and amplitude of the ipsilateral hemidiaphragm was expressed as a percentage of the contralateral hemidiaphragm.

2.9. Tissue processing

Seven weeks post-surgery, under deep isoflurane anesthesia animals were transcardially perfused with 60 ml of ice-cold 0.1 M phosphate-buffered solution (PBS) followed by 4% paraformaldehyde in PBS (Sigma-Aldrich, St. Louis, MO, USA). Subsequently the cervical spinal cords were post-fixed overnight in 10% sucrose in PFA at 4 °C and then cryoprotected in 30% sucrose in PBS at 4 °C for 24 h. A two centimeter spinal cord section from C1 to C7 was embedded in optical cutting temperature (OCT) matrix and transversely sectioned at 40 μm thickness with freezing microtome from 3000 μm rostral to 15,000 μm caudal to the hemisection epicenter and stored at −80 °C.

2.10. Immunohistochemistry

Neuroprotection caudal to high cervical hemisection was assessed using ChAT positive ventral horn motoneurons. Sections were washed

(three times for 5 min) in 0.1 M PBS and blocked in 0.1 M PBS containing 5% nonfat milk, 1% BSA, and 0.3% Triton X-100 for 1 h. Sections were first incubated overnight at 4 °C in primary mouse ChAT antibody (Millipore; 1:100) and subsequently washed in PBS and incubated with secondary antibody in blocking solution with 0.3% Triton-X. A Biotin–Avidin complex (ABC kit, Sigma-Aldrich) was used to conjugate and reacted with 0.05% 3,3″-diaminobenzidine hydrogen peroxide for 3–15 min for visualization. Finally, the sections were washed in PBS, dehydrated and covered with mounting medium. Motoneurons within the ipsilateral and contralateral ventral horns were quantified using unbiased stereology.

2.11. Immunofluorescence

Overall changes in synapses in the ventral horn were examined using antibodies directed at synaptophysin (1:50; Millipore). Specific alterations in glutamate receptor expression were detected with the NMDA receptor subunit (NR2A, 1:100; Millipore) and AMPA receptor subunit (GLUR1, 1:100). Motoneurons were probed by overnight incubation at 4 °C with mouse anti-choline acetyltransferase (ChAT, 1:100; Millipore) in blocking solution. Sections were incubated overnight with primary antibodies. The slides were then washed three times with PBS and incubated with fluorescent Alexa 488, 588 or 647 secondary antibodies (1:500, Invitrogen). The slides were finally coverslipped with Mowiol which contained the fluorescent anti-nuclear stain 4′,6-diaminidino-2-phenylindone (DAPI).

2.12. Stereological quantification

Ventral horn motoneuron counts were completed using unbiased stereological quantification. For this quantification, a total of 10 mm of tissue between C3 and C8 was sampled at every tenth section beginning at a random starting point chosen by the random number generator on the StereoInvestigator software. The optical fractionator sampling probe of the software was used for workflow creation and sampling design. On each section quantified, the ipsilateral and contralateral dorsal and ventral horns were separately traced. For each tracing, a systematic random set of samples measuring 200 × 200 mm was generated. The optical fractionator's unbiased counting frame for all counts was 100 × 150 mm. The thicknesses of the sections were measured using the software and the average thickness was reduced to 80% of the original thickness. Using the optical fractionator's workflow probe, immunostained cells that fell within or on inclusion lines of the sampling frame were considered neurons. The settings used to complete stereological counts were: 1/section sampling factor = 15, 1/area sampling factor = 2.78, tissue sampling factor (TSF) = 0.78, guard zone = 6 μm.

2.13. Statistical analysis

All statistical analysis was computed using SigmaStat software. Groups were compared using Student's t-test, one-way ANOVA tests, and two-way repeated-measures ANOVA tests followed by post-hoc analysis using Bonferroni's test as indicated. Data presented in the results are mean $+/-$ SEM unless otherwise indicated. Values of $p < 0.05$ were considered to be significant.

3. Results

3.1. Riluzole restores synaptic input onto cervical motoneurons following C2 hemisection injury

In uninjured sham animals, synaptophysin expression was found to be distributed in the cervical spinal gray matter as well as through the white matter (Fig. 2). Synaptophysin immunoreactivity was intensely aggregated on the soma and dendrites within lamina 1×. The effects
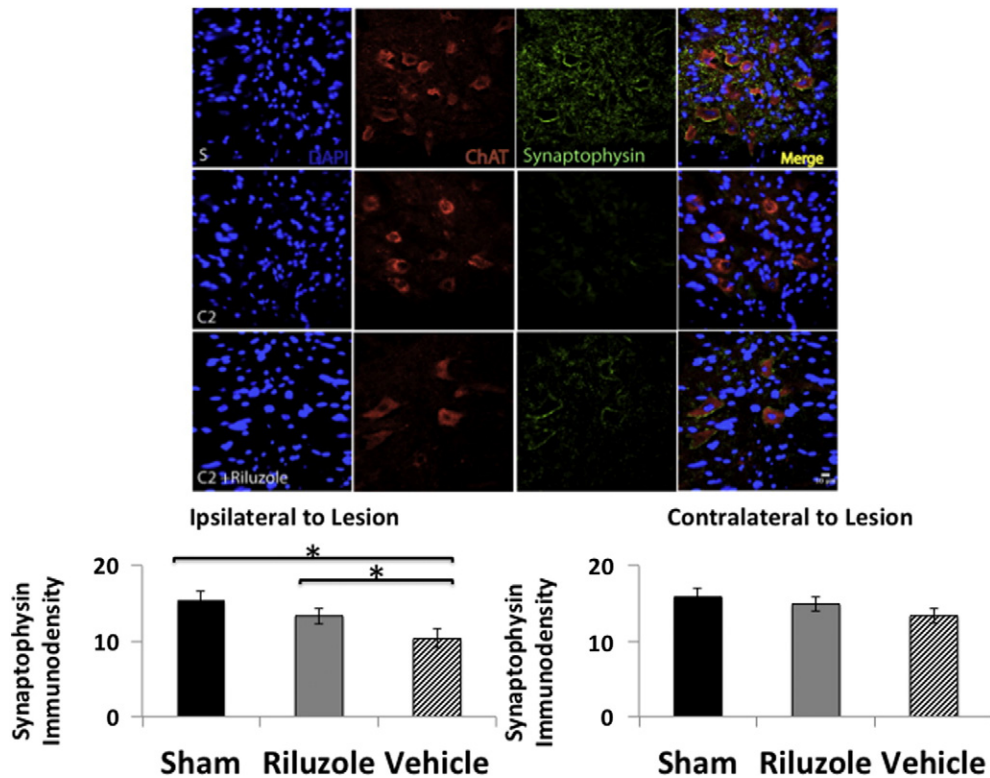
Fig. 2. Synaptophysin immunostaining in cervical spinal cord ventral horn 6 weeks after left C2 hemisection and riluzole treatment. Cervical spinal cord sections from sham, injured and injured animals treated with riluzole were stained with the nuclear marker DAPI (blue), ChAT (red) and synaptophysin (green). Top panel demonstrates synaptophysin immunolabeling in a sham animal associated with ventral horn motoneurons labeled with ChAT. The bottom two panels show significantly more preservation of synaptophysin labeling on the surface of lesioned motoneurons treated with riluzole compared to vehicle treated controls. Quantification of immunolabeling revealed no significant difference on the contralateral uninjured side.

of C2 spinal hemisection injury and riluzole treatment on the caudal cervical ventral horn synaptophysin immunofluorescence levels were significant (one way ANOVA, p < 0.001). Six weeks after left C2 spinal cord hemisection, synaptophysin expression level on the left cervical spinal cord was 10.31 + 1.11 and 13.46 + 1.05 in vehicle and riluzole treated groups, respectively. Synaptophysin expression was significantly lower in both injured groups compared to sham injured animals (p < 0.001). However, synaptophysin expression levels on the contralateral side of the injured cervical spinal cord were not altered in injured groups compared to sham animals. Riluzole treated group had a significantly elevated levels of synaptophysin on the injured side of the cervical spinal cord compared to injured animals treated with vehicle. This elevated level of synaptophysin expression was found on ChAT positive ventral horn motoneurons with dendritic projections associated with synaptophysin positive terminals.

3.2. Riluzole treatment was associated with increased NR2A and GLUR1 expression ipsilateral to the injury

Alterations in specific AMPA and NMDA receptor subunits were assessed. Specifically, alterations in the NR2A subunit of the NMDA receptor were examined to demonstrate lasting changes in synaptic efficacy. NR2A and GLUR1 immune reactivity was seen associated with neurons in the anterior horn of cervical spinal cord caudal to the injury. In the caudal cervical region, ipsilateral to the injury, NR2A levels were significantly decreased compared to the corresponding region in the
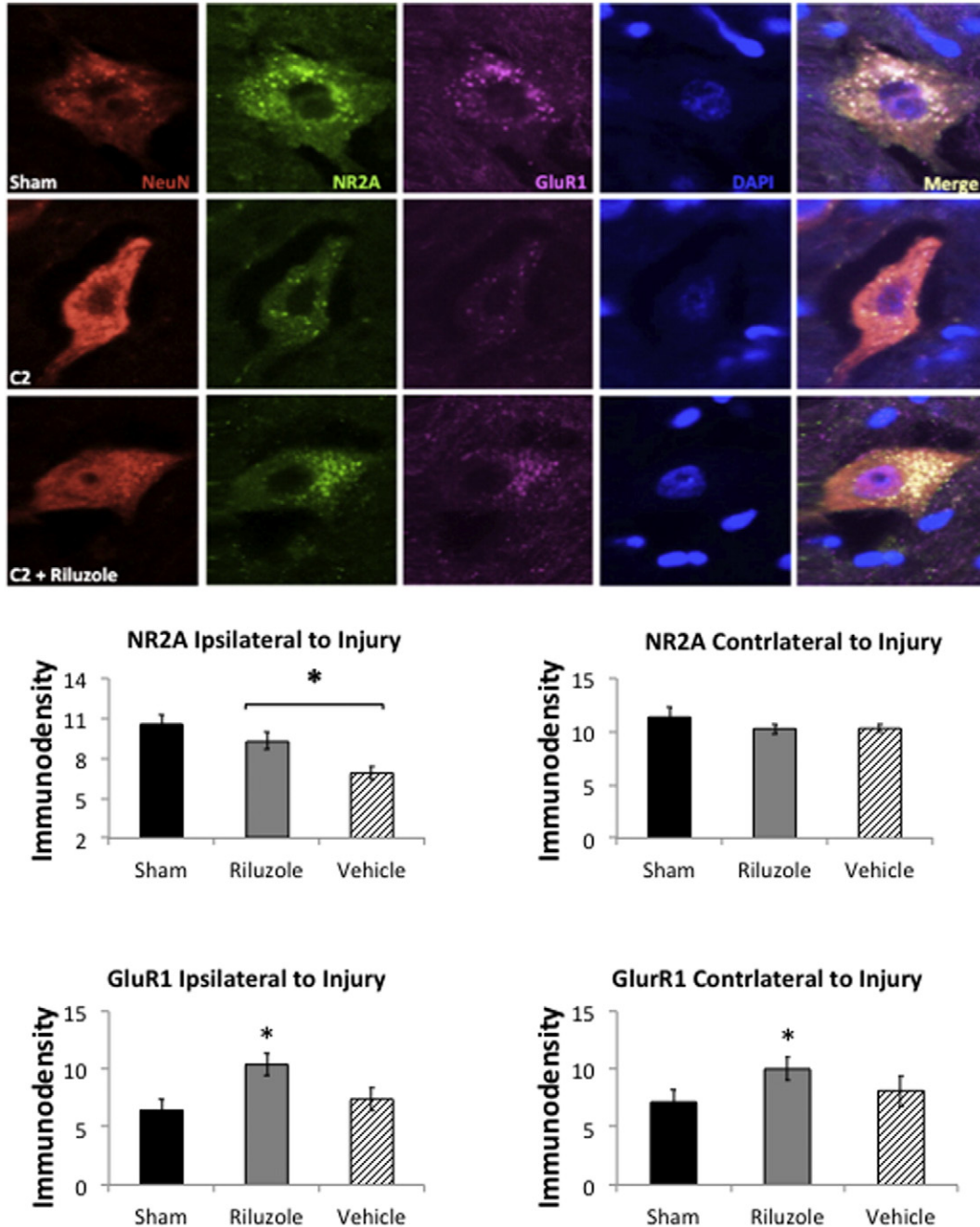

Fig. 3. At 6 weeks after left C2 hemisection injury, immunostaining demonstrates that expression of the NR2A subunit of the NMDA receptor and the GLUR1 subunit of the AMPA receptors associated with ventral horn motoneurons were significantly enhanced in the riluzole treated animals compared to controls. While, NR2A increase was only seen on the side ipsilateral to the injury GluR1 subunit was upregulated bilaterally in the riluzole treated animals (p < 0.05).

sham group (p < 0.01) (Fig. 3). Treatment with riluzole after injury resulted in significantly attenuating this decrease, with the treated group showing no significant decrease compared to the uninjured group. Comparison of NR2A levels between the injured groups showed a significantly greater level in the riluzole treated group compared to the vehicle treated group (p < 0.05).

Secondly, this part of the study addressed the question of whether synapses containing NR2A receptors also contained the Ca^{2+} impermeable AMPA receptors composed of GLUR1 subunits. We found that NR2A immunoreactive punta on vernal horn neurons were colocalized with GLUR1 immunoreactivity. Colocalization of these subunits was examined in quadruple labeled sections (Fig. 3). There was extensive colocalization of NR2A, GLUR1 and NeuN. As such, the immunofluorescence level of GLUR1 followed that of NR2A in the three different experimental groups examined. That is to say, the significant decrease in GLUR1 immunoreactivity following injury was returned to control levels as a result of riluzole treatment (Fig. 3).

3.3. Riluzole increases ipsilateral motoneuronal excitability following high cervical hemisection

In order to evaluate the excitatory state of the cervical spinal circuitry innervating the forelimb that could underlie the mechanism of functional recovery, an analysis of the H-response was carried out at various stimulation frequencies. The H- and M-waves were obtained by stimulating the

radial nerve and recording muscle response from the extensor carpi radialis muscle. Direct M-wave, which is the orthodromically activated muscle response, and the recurring H-wave were consistently reproducible with similar morphology in sham and both of the injured groups (Fig. 4). The H-wave represents the persistent output from antidromically-stimulated motor neurons (Milanov, 1992; Fisher, 1992). In particular, H-wave amplitude has been shown to be a measure of spinal motoneuron excitability. There were no differences in H- and M-wave latency between the three groups indicating a lack of peripheral nerve involvement following injury or treatment (Fig. 4A). The stimulus intensity required to elicit M-wave was much lower compared to the threshold intensity required to evoke the H-wave (data not shown). Maximal M-wave was also achieved at a lower stimulus intensity compared to that required for the maximal H-response. The ratio of maximal H-wave to maximal M-wave was compared at stimulation intensity that evoked maximal H-wave without depressing M-wave at increasing stimulation frequencies (Fig. 4). Increasing the stimulation frequency from 0.2 to 10 Hz did not alter the amplitude of the direct muscle response but had a significant depressive effect on the H-response from both the ipsilateral and contralateral neuronal circuitry. This frequency dependent depression was seen bilaterally in all three experimental groups. C2 hemisection injury resulted in a significant decrease in the excitability of ipsilateral cervical spinal circuitry at 0.2 Hz, 1 Hz, 5 Hz and 10 Hz stimulation frequencies (p < 0.05). Riluzole-treatment following this high cervical SCI led to the restoration of
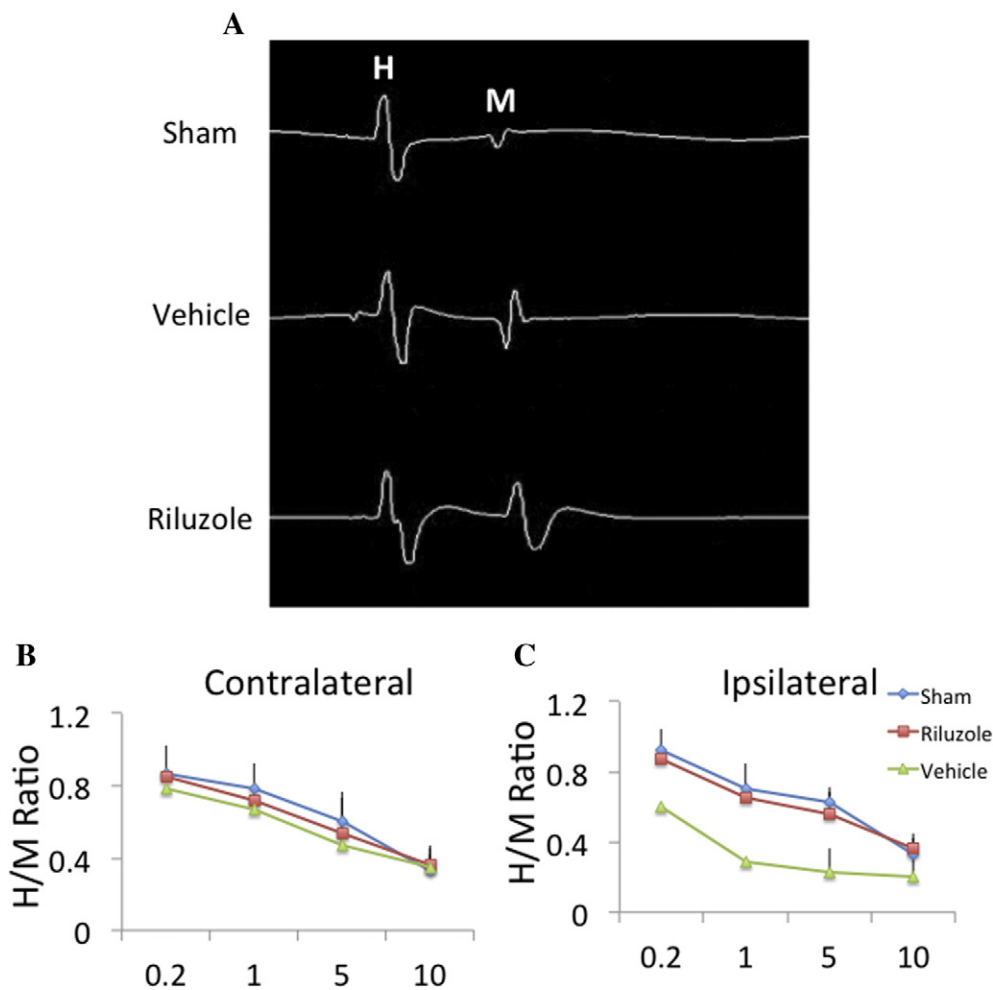
Fig. 4. Riluzole treatment results in recovery of ventral horn excitability (A) Representative waveforms of Hmax/Mmax waves in injured, riluzole treated, and non-injured animals. (B) Results shown are the rate-dependent depression of H/M tested at 0.2, 1, 5, and 10 Hz. At 6 weeks after C2 hemilesion injury there are no differences in contralateral forelimb H/M between control and riluzole treated animals. (C) At 6 weeks after C2 hemisection injury, ipsilaterally, vehicle treated animals show reduced H/M at all frequencies tested compared to that of riluzole and control treated animals (p < 0.05 at all frequencies).
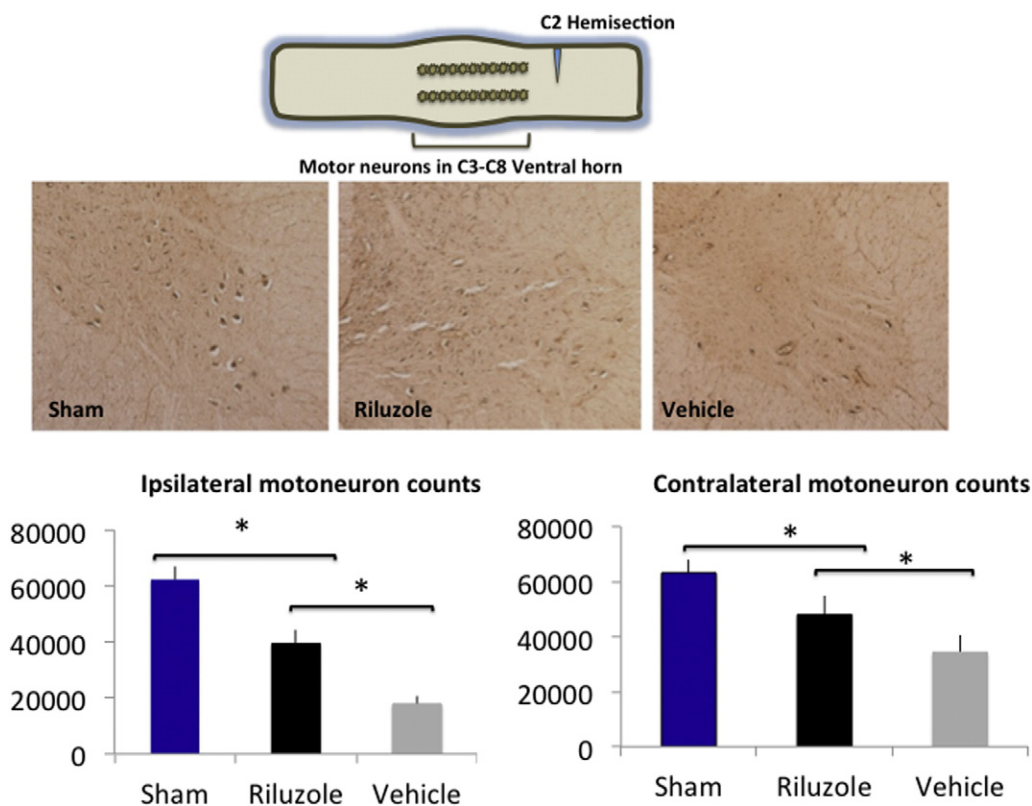
Fig. 5. Measure of Choline Acetyltransferase (ChAT) positive cells within 10 mm long cervical spinal cord containing presumptive PMNs and forelimb specific motoneurons using unbiased stereology. Motoneuron counting was significantly reduced in the injured group compared to sham animals bilaterally. Riluzole treated animals had significantly more cervical motoneurons bilaterally compared to vehicle treated animals (p < 0.05).

Hmax/Mmax ratios to ratios equivalent to those in sham animals. Injury alone or injury in combination with riluzole administration did not affect the Hmax/Mmax ratios obtained from the contralateral forelimb.

3.4. Riluzole attenuates motoneuronal loss following C2 hemisection injury

Loss of excitatory supraspinal input combined with a decrease in spinal inhibitory input can lead to changes in the number of motoneurons caudal to the injury. Examination of the ventral horn motoneurons within an 8 mm cervical spinal segment containing the forelimb and respiratory circuitry revealed a significant reduction in the number of ChAT-positive motoneurons ipsilateral (p < 0.001) and contralateral (p < 0.05) to the injury compared to same spinal areas in the sham injured spinal cord (Fig. 5). The reduction was significantly more pronounced on the side ipsilateral to the injury compared to the contralateral side. With the initiation of riluzole treatment at 1 h following injury,

the injury-induced reduction in the number of motoneurons was starkly dampened on both ipsilateral and contralateral sides of the injury. The riluzole treatment-induced effect was seen on both the left and right sides of the spinal cord with the riluzole-treated group having significantly more ventral horn motoneurons compared to the vehicle-treated group. To further validate the significant loss of motoneurons within the cervical enlargement caudal to the left C2 hemisection injury, a left C2 hemisection was carried out in ChAT-eGFP transgenic mice and examined the spinal cord from C1 to T3 for expression of eGFP in cholinergic neurons (Fig. 6). Initial, confocal imaging of the cervical spinal cord sections from left C2 hemisected ChAT-eGFP mice demonstrated a decreased eGFP positive neurons in the ipsilateral anterior horn of the gray matter compared to the contralateral side. To fully appreciate the region and extent of motoneuron loss, we performed 3D reconstruction of the spinal cord tissue from ChAT-eGFP mice after left C2 hemisection using the Stereoinvestigator software. This detailed work clearly and
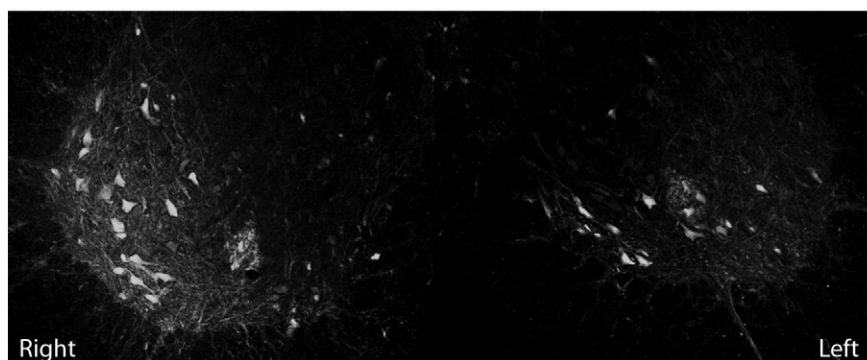
Fig. 6. Loss of cervical ventral horn motoneurons following left C2 hemisection. Photomicrograph shows a representative cervical spinal cord section at C5 from a ChAT-eGFP mice 6 weeks after left C2 hemisection injury. This clearly demonstrates and validates our reported loss of ventral horn motoneurons caudal and ipsilateral to a left C2 hemisection injury.

elegantly demonstrates that the motoneuronal loss is restricted to a specific area of the cervical enlargement where majority of the respiratory and forelimb motoneurons are located (Fig. 7).

3.5. Riluzole promotes recovery of forelimb and forepaw function following high cervical hemisection injury

Riluzole treatment following high cervical spinal cord hemisection injury elicited early recovery of ipsilateral forelimb grip strength while the contralateral forelimb recovery emerged much later. High cervical hemisection injury resulted in significant deficits in ipsilateral forelimb grip strength, evident as early as one day post-injury (Fig. 8a). Contralateral forelimb also displayed significant loss in grip strength but to a much lesser extent compared to the ipsilateral forelimb (Fig. 8b). Both forelimbs showed spontaneous recovery of function over time, with riluzole treated animals showing significant recovery of ipsilateral grip strength as early as 3 days post-injury compared to vehicle treated animals ($p < 0.01$). Riluzole-mediated recovery of contralateral forelimb grip strength occurred much later, at 23 days post-injury, compared to vehicle treated controls ($p < 0.01$). Functional recovery of both forelimbs persisted at 6 weeks post-injury. Riluzole elicited recovery of ipsilateral grip strength above the spontaneous recovery seen in the vehicle-treated control animals, which plateaued by 11 days after injury.

Using CatWalk gait analysis, we found that, at 2 weeks post-injury, the swing speed was significantly different amongst the treatment groups with the riluzole treated group having greater swing speed ($p < 0.005$) (Fig. 9). This difference persisted at both 4 and 6 weeks ($p < 0.05$), however at 6 weeks the difference did not reach significance. The riluzole treated group had swing speeds of 0.43 ± 0.02 mm/ms, $0.55 + 0.05$ mm/ms, and $0.5 \pm 0.$ mm/ms, at 2, 4 and 6 weeks respectively. In comparison the vehicle treated group had swing speeds of 0.32 ± 0.02 mm/ms, 0.42 ± 0.02 mm/ms and 0.38 ± 0.06 mm/ms at 2, 4 and 6 weeks, respectively. Similarly, ipsilateral stride length was different between the riluzole treated and vehicle treated groups at 2 and 4 weeks post-injury ($p < 0.001$ and $p < 0.008$). At 6 weeks post-injury, the difference in stride length between the riluzole treated group and vehicle treated control did not reach significance ($p = 0.197$).

Animals that had been subjected to sham injury did not display preferential use of a single paw. In the first week following injury, animals in the control group that had been treated with vehicle solution used the contralateral paw preferentially while exploring the cylinder whereas the ipsilateral forepaw was held close to the body and the animals were unable to make placements on the wall (Fig. 10). Number of paw placements made with both paws simultaneously and/or the use of ipsilateral forepaw were significantly more in the injured animals treated with riluzole compared to vehicle treated controls ($p < 0.05$). In line with these results CatWalk analysis revealed that the forepaw print width during stance phase was significantly increased in the riluzole treated animals compared to control animals at 2, 4 and 6 weeks post-injury ($p < 0.01$, $p = 0.005$ and $p = 0.005$, respectively). Specifically, in the riluzole treated group the forepaw print width was 14.17 ± 0.32 mm, 13.65 ± 0.23 mm and 13.6 ± 0.57 mm at 2, 4 and 6 weeks post-injury. The vehicle treated group had print widths of 12.42 ± 0.51 mm, 9.57 ± 0.78 mm and $10.1 + 0.35$ mm at the above time points. In addition, ipsilateral print lengths of riluzole treated animals at 2, 4 and 6 weeks were $16.00 + 0.51$ mm, 16.53 ± 0.80 mm and 18.23 ± 1.20 mm respectively. Those of vehicle treated animals were 12.42 ± 0.31 mm, 13.06 ± 0.42 mm and 14.96 ± 0.45 mm at 2, 4 and 6 weeks respectively. Print length of the ipsilateral forepaw in control animals was significantly lower than those of the treated animals at 2, 4 and 6 weeks ($p < 0.005$, $p < 0.005$ and $p < 0.05$, respectively). However, the print width and length of the contralateral forepaw were not significantly different between treatment groups. On the ipsilateral side, the print width was similar at all three time points while the
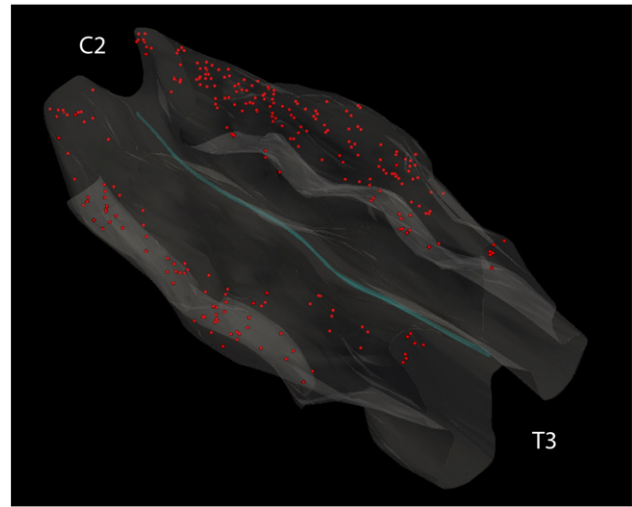

Fig. 7. ChAT positive neurons were mapped using Neurolucida to create a 3D reconstruction of the spinal cord from the site of injury at C2 rostrally to T3 caudally.

vehicle treated animals showed a significant decline in print width at both 4 and 6 weeks compared to the initial measurement at the 2 weeks post-injury time.
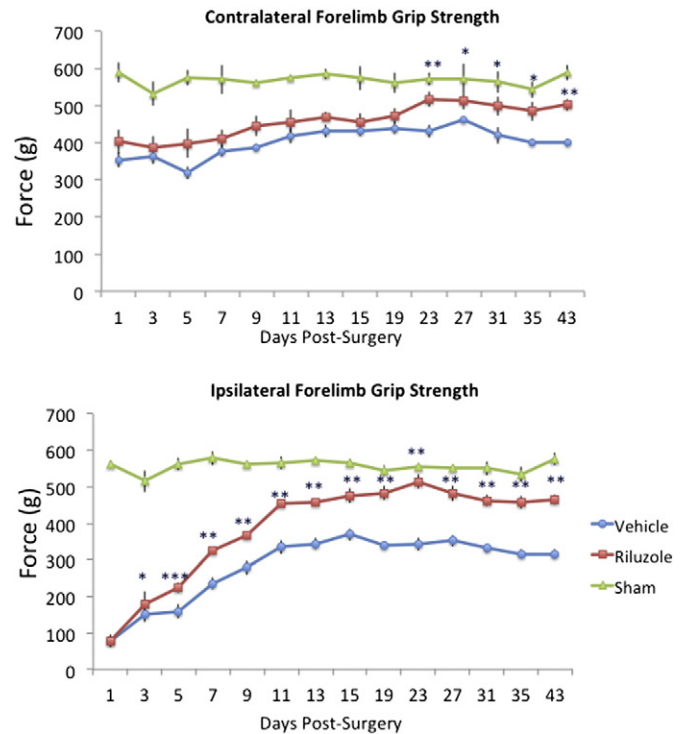

Fig. 8. Riluzole promotes early and sustained plasticity resulting in ipsilateral and contralateral forelimb motor recovery. Immediately after cervical (C2) spinal cord hemisection, ipsilateral grip strength was significantly decreased. Injured rats displayed spontaneous recovery of grip strength ability that plateaued at 15 days post-injury. Both riluzole and vehicle treated animals displayed recovery of ipsilateral grip strength over the tested period. Riluzole treated animals displayed significantly greater recovery of ipsilateral grip strength compared to vehicle treated animals as early as 5 days post-injury. The riluzole-mediated recovery was sustained (two-way ANOVA, $p < 0.01$ for all time points). Contralateral forelimb grip strength was also significantly decreased after injury. Riluzole promoted delayed recovery of contralateral grip strength at day 23 post-injury (2-way ANOVA, $p < 0.001$ at all time points).

3.6. Riluzole increased the proportion of animals displaying diaphragmatic functional recovery following high cervical hemisection injury

Diaphragmatic EMG was recorded from a subset of animals under anesthesia at 2 weeks post-C2 hemisection to determine the proportion of animals that showed recovery of ipsilateral hemidiaphragm EMG activity during eupnea. At two weeks post-injury, some animals that had been injured showed recovery of ipsilateral diaphragmatic function that was rhythmic and synchronous with the intact contralateral hemidiaphragm (Fig. 11A). Two weeks after injury, 2 out of 9 vehicle treated animals (22.2%) showed recovery of ipsilateral hemidiaphragm EMG activity (Fig. 11B). Riluzole treatment following cervical injury led to an increase in the percentage of animals that showed ipsilateral diaphragmatic recovery, with 5 out of the 6 animals (83.3%) showing recovery.

The extent of ipsilateral hemidiaphragm EMG recovery was determined by calculating the peak inspiratory burst amplitude from raw EMG tracings in only those that displayed recovered respiratory activity.

Riluzole treatment significantly enhanced the extent of respiratory related activity on ipsilateral hemidiaphragm ($p < 0.05$). In vehicle treated animals that showed recovery, peak inspiratory amplitude was $25.95 \pm 1.24\%$ of the contralateral side of the same animal. In riluzole treated animals the peak inspiratory burst amplitude was $55.07 \pm 5.84\%$ of the contralateral side.

4. Discussion

This study demonstrates that C2 hemisection injury results in decreased excitability and most importantly, for the first time demonstrates a significant loss of motoneurons within the caudal cervical spinal cord housing the forelimb and respiratory spinal networks. Further, we demonstrate that acute and subacute riluzole administration upregulates GLUR1 and NR2A subunits of AMPA and NMDA receptors, and enhances motoneuronal excitability. Most importantly, riluzole had a significant impact in minimizing this loss of motoneurons residing
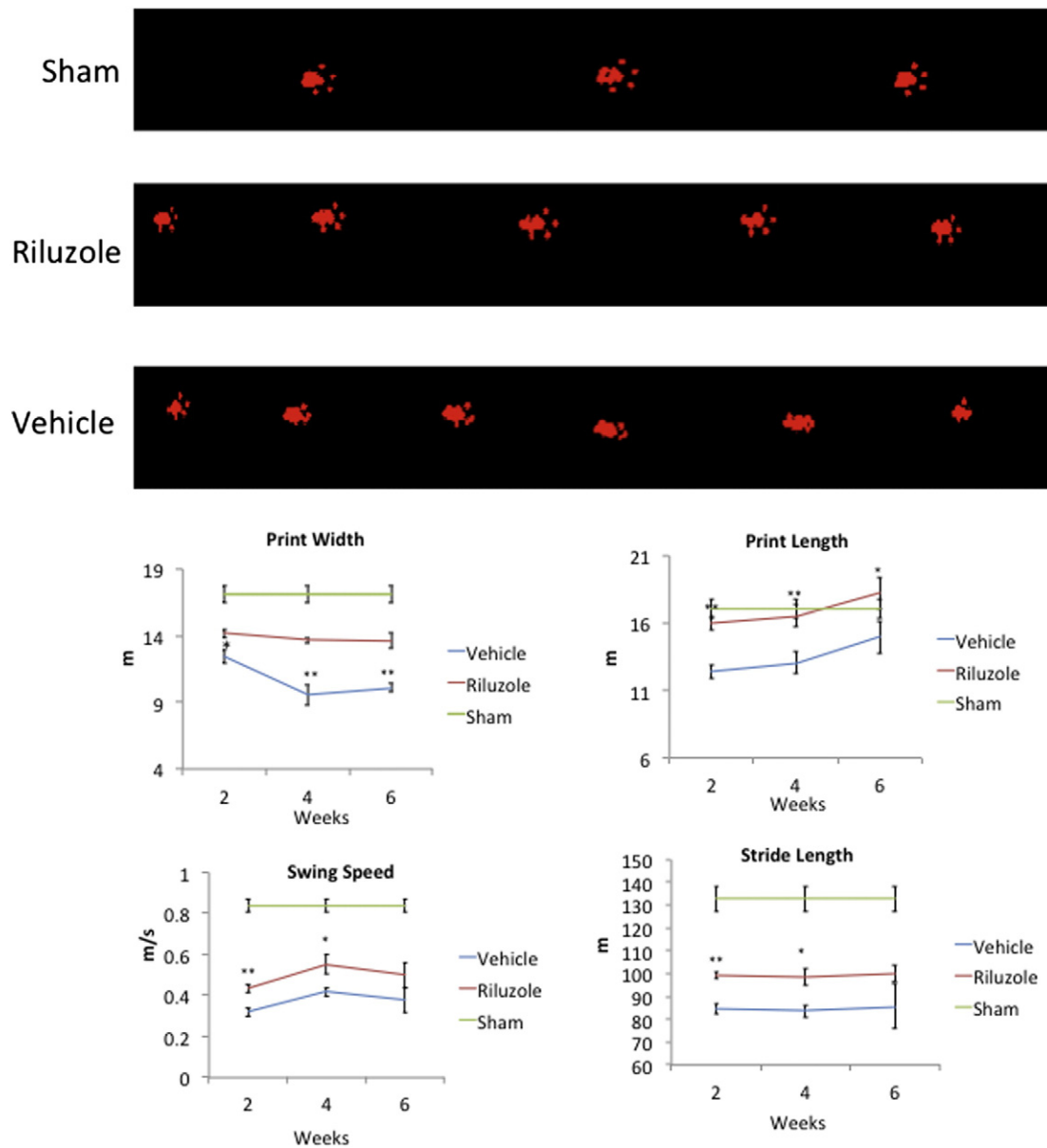
Fig. 9. Riluzole treatment results in sustained improvement of forelimb and forepaw function after C2 hemilesion injury. Representative ipsilateral forelimb tracings of gait in control and riluzole treated animals. Riluzole results in increased stride length at weeks 2 and 4 post surgery ($p < 0.001$ and $p = 0.008$ respectively). Riluzole results in increased print length at weeks 2 and 4 post surgery ($p = 0.003$ for both time points). Riluzole results in greater swing speed measured at weeks 2 and 4 post surgery ($p = 0.005$ and $p = 0.022$). Riluzole treatment results in increased stride length at weeks 2 and 4 post surgery ($p < 0.001$ and $p = 0.008$).

caudal to C2 hemisection. Finally, these results were also linked to significant forelimb and respiratory motor recovery.

Protection of spinal tissue can be a significant mediator of functional recovery following SCI and it has been demonstrated that even a small amount of preserved tissue can lead to substantial functional recovery through neuroplasticity of the remaining tissue. Glutamate levels are significantly increased within the spinal cord following SCI (Panter et al., 1990) and dysregulation of glutamate transmission and over-activation of glutamate receptors are detrimental to neural tissue at the site of injury (Xu et al., 2004, 2008). One strategy for minimizing the secondary injury and preserving tissue in the injured spinal cord involves minimizing this rapid and immediate decrease in intraspinal glutamate levels. Indeed, our laboratory and others have previously demonstrated that the antiglutamatergic effects of riluzole can provide neuroprotection at and around the site of initial injury (Wu et al., 2013, 2014; Schwartz and Fehlings, 2001, 2002; Karadimas et al., 2013; Mu et al., 2000; Wilson et al., 2013; Mazzone and Nistri, 2011; Lang-Lazdunski et al., 2000; McAdoo et al., 2005; Moon et al., 2014; Stutzmann et al., 1996). Although riluzole promotes modest motor recovery in preclinical models of SCI, the exact mechanisms of action remain unclear limiting our ability to fully harness its therapeutic potential for SCI. Here, we have used a C2 hemisection injury model in order to explore the capacity of riluzole to promote sustained neuroplasticity.

Organization and functionality of the spinal cord are determined, to a large extent, by the diversity of neuronal populations and their connectivity. Following acute SCI, main axonal pathways transporting glutamatergic input onto the ventral horn motoneurons are disrupted (Shapiro, 1997). The majority of research to date, utilizing the established C2 hemisection model of incomplete SCI, has focused on promoting plasticity within the spared spinal circuitries to bring about functional recovery (Mantilla et al., 2013; Baker-Herman et al., 2004; Golder et al., 2003; Ling et al., 2001). Specifically, acute and chronic interventions using pharmacological agents and intermittent hypoxia training have been used to activate latent axonal pathways that cross the spinal cord below the injury to promote functional plasticity (Baker-Herman et al., 2004; Li et al., 2014; Nantwi and Goshgarian, 2001; Dale-Nagle et al., 2010; MacFarlane et al., 2011). However, little attention has been paid to the survival of the motoneuronal elements that comprise these circuitries located caudal to the C2 hemisection and subsequently to the development of therapies targeted at limiting this loss (Alilain and Goshgarian, 2007, 2008; Goshgarian, 2003; Zimmer and Goshgarian, 2005; Fuller et al., 2009; Agrawal and Fehlings, 1997; Baker-Herman et al., 2010). Here, we show that the C2 hemisection injury results in decreased descending input onto motoneurons leading to significant loss of motoneurons located distal to the initial injury. For the first time, we provide evidence not only suggesting motoneuron loss caudal to the C2 hemisection injury but also supporting riluzole treatment as a potential means to limit this loss.

Various ionotropic glutamate receptor subunits are strongly implicated in the induction and maintenance of neuroplasticity within the central nervous system. Of the three types of ionotropic glutamate receptors, NMDA and AMPA receptors have been shown to alter in response to neuronal activity. The type of glutamate subunits that combine to form the glutamate receptor influences the firing property of motoneurons (Myers et al., 1999; Dingledine et al., 1999). AMPA receptor composition can have a significant impact on motoneuronal excitability while NMDA receptors function as coincidence detectors to strengthen weak synaptic connections (Evans et al., 2012). In particular, increased expression of the GLUR1 subunit of the AMPA receptor and the NR2A subunit of the NMDA receptor have been strongly linked to synaptic strengthening associated with LTP, the cellular substrate of learning and memory, as well as respiratory plasticity (Alilain and Goshgarian, 2007, 2008; Lee et al., 2000; Mitsushima et al., 2011; Shao et al., 2003). Loss of descending activity following SCI has been linked to changes in the expression of NMDA and AMPA receptor subunits

(Mantilla et al., 2012; Alilain and Goshgarian, 2008; Grossman et al., 1999, 2000; Anderson et al., 2005). In the setting of SCI, modulation of both NMDA and AMPA receptors has been previously shown to mediate neuroplasticity within the cervical spinal cord following C2 hemisection injury (Mantilla et al., 2012; Alilain and Goshgarian, 2008). Indeed, this is supported by our findings of an increase in NR2A and GLUR1 subunits in the cervical ventral horn and the increase in motoneuronal excitability in the riluzole treated group.

Based on the literature (Sim et al., 2013; Bacci et al., 2001; Gomperts et al., 1998, 2000; Malenka, 2003; Nicoll and Malenka, 1999; Grooms et al., 2006) riluzole-mediated increase in cervical motoneuron excitability could promote synaptic strengthening through modification of pre- and postsynaptic neuronal properties. Indeed, we found a concomitant increase in the presynaptic input onto the motoneurons of the riluzole treated group as measured by the increased synaptophysin expression on the ChAT positive cells in the anterior horn of gray matter. Taken together, these findings suggest that the ability of riluzole to modulate glutamate receptor expression has the potential to influence pre-and post-synaptic membranes to enhance synaptic strength and to amplify excitability and functional plasticity of preserved motoneurons within distal spinal motoneurons. This activity-dependent increase in the presynaptic input could underlie the survival, connectivity and function of the motoneurons and provide novel mechanistic insights into the effects of riluzole following injury in the CNS.

SCI patients place high priority on regaining arm and hand function (Alexander et al., 2009) as well as on acquiring ventilator independence for enhanced quality of life, making these functional improvements of paramount importance in SCI research (Anderson et al., 2005). Pulmonary complications such as infection, atelectasis and ventilator dependence due to hypoventilation are the leading causes of death amongst SCI patients (Kelley et al., 2003). Our neurobehavioral results verify previous findings that riluzole treatment leads to neurobehavioral improvements (Wu et al., 2013, 2014; Schwartz and Fehlings, 2001; Anon., 2003; Baptiste and Fehlings, 2006) and extends the findings relating to the benefits of riluzole by providing evidence for riluzole's ability to bring forth early and sustained forelimb functional recovery and restore respiratory related diaphragmatic function. In this study we have used diaphragmatic EMG recordings in spontaneously breathing animals to assess respiratory recovery. We were able to maintain comparable conditions in all groups. Further, we did not find a difference in respiratory frequency between the riluzole and vehicle groups indicating a similar respiratory drive in both groups. This riluzole-mediated early forelimb functional recovery following high cervical SCI has never been demonstrated previously and this study provides evidence

Ipsilateral forepaw placements during cylinder exploration
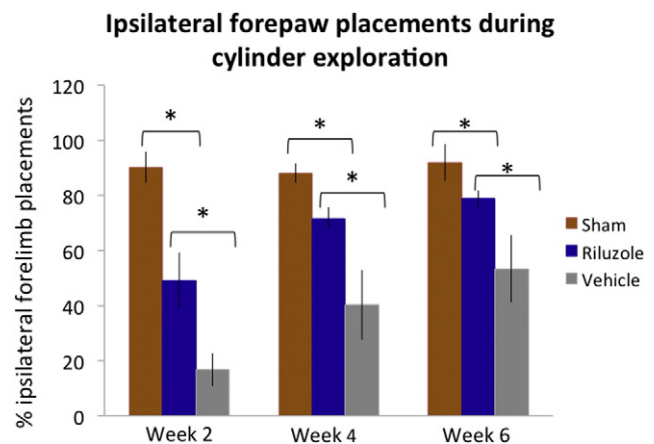
Fig. 10. The number of forelimb placements (left, right, and both) on the cylinder was counted and expressed as a percentage of total placements. Percentage of ipsilateral paw placements was significantly higher in the C2 hemisected animals treated with riluzole compared control animals receiving vehicle solution (2-way ANOVA, p < 0.001 at all time points).
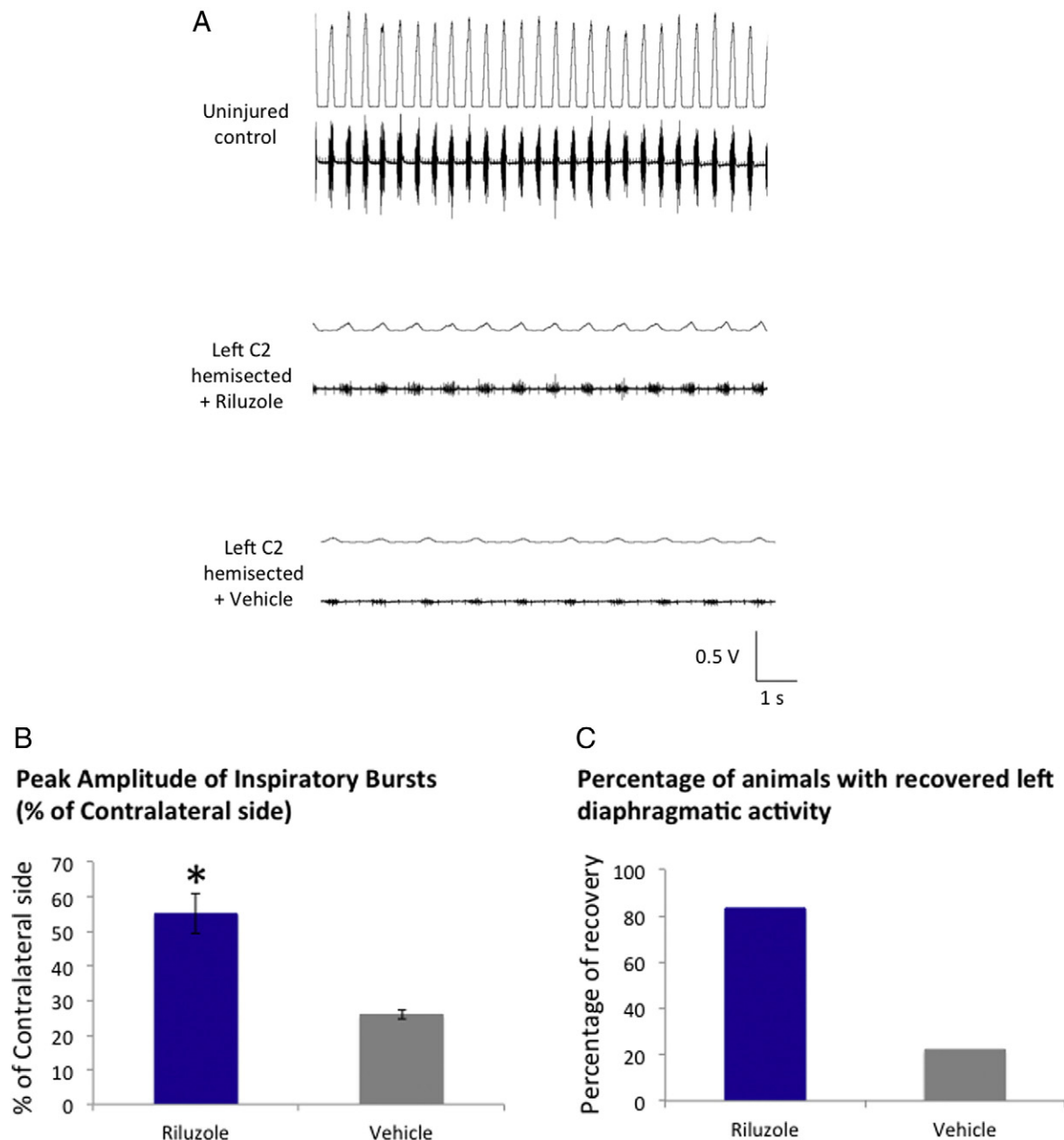
Fig. 11. Diaphragmatic EMG assessment. (A) Representative raw left hemidiaphragmatic EMG and integrated EMG activity taken from uninjured, left C2 hemisected animal treated with riluzole or vehicle two weeks post-injury. (B) Four out of the 5 riluzole treated animals had recovery of respiratory related diaphragmatic activity on the lesioned side. At two weeks, a higher percentage of animals that received riluzole had recovery of hemidiaphragmatic function on the lesioned side. (C) The riluzole treated animals had a higher peak inspiratory burst amplitude compared to the vehicle treated group (t-test, $p < 0.05$).

of this using multiple outcome measures. In conjunction with the neuro-anatomical findings, our findings of early recovery of ipsilateral gripping ability at three days post-injury further suggest that neuroplasticity rather than regeneration is the underlying mechanism of recovery. Although there is limited existing evidence for the potential role of riluzole in functional plasticity, the findings of this study suggest a glutamate receptor antagonism-mediated homeostatic plasticity similar to what has been reported with other glutamate modulators in the respiratory and locomotor networks (Mantilla et al., 2012; Alilain and Goshgarian, 2007, 2008). Unlike the other modulators, the proven safely record of riluzole in the clinical setting makes it an attractive option.

The findings presented here indicate that the acute administration of riluzole for a week post-injury is a potential approach to promote neuroprotection of caudal neural circuitries responsible for forelimb and respiratory function. Although therapeutic benefits of riluzole

have been demonstrated in other models of SCI, the use of the C2 hemisection model allowed us to demonstrate its potential effect on synaptic input and number of motoneurons located caudal to the site of injury. In fact, this study demonstrates the effectiveness of a drug that can improve two of the most devastating consequences of SCI, impaired forelimb and respiratory function. As this drug is currently in Phase III trials, this work is expected to have an impact for the treatment of SCI.

Public Benefit Foundation. The funding sources had no role in the study design; in the collection, analysis and interpretation of data; in the writing of the report; or in the decision to submit the article for publication.

References

Agrawal, S.K., Fehlings, M.G., 1997. The effect of the sodium channel blocker QX-314 on recovery after acute spinal cord injury. J. Neurotrauma 14 (2), 81–88.

Alexander, M.S., et al., 2009. Outcome measures in spinal cord injury: recent assessments and recommendations for future directions. Spinal Cord 47 (8), 582–591.

Alilain, W.J., Goshgarian, H.G., 2007. MK-801 upregulates NR2A protein levels and induces functional recovery of the ipsilateral hemidiaphragm following acute C2 hemisection in adult rats. J. Spinal Cord Med. 30 (4), 346–354.

Alilain, W.J., Goshgarian, H.G., 2008. Glutamate receptor plasticity and activity-regulated cytoskeletal associated protein regulation in the phrenic motor nucleus may mediate spontaneous recovery of the hemidiaphragm following chronic cervical spinal cord injury. Exp. Neurol. 212 (2), 348–357.

Anderson, D.K., et al., 2005. Recommended guidelines for studies of human subjects with spinal cord injury. Spinal Cord 43 (8), 453–458.

Anon., 2003. Dosage effects of riluzole in Huntington's disease: a multicenter placebo-controlled study. Neurology 61 (11), 1551–1556.

Bacci, A., et al., 2001. Chronic blockade of glutamate receptors enhances presynaptic release and downregulates the interaction between synaptophysin–synaptobrevin–vesicle-associated membrane protein 2. J. Neurosci. 21 (17), 6588–6596.

Baker-Herman, T.L., et al., 2004. BDNF is necessary and sufficient for spinal respiratory plasticity following intermittent hypoxia. Nat. Neurosci. 7 (1), 48–55.

Baker-Herman, T.L., et al., 2010. Differential expression of respiratory long-term facilitation among inbred rat strains. Respir. Physiol. Neurobiol. 170 (3), 260–267.

Baptiste, D.C., Fehlings, M.G., 2006. Pharmacological approaches to repair the injured spinal cord. J. Neurotrauma 23 (3–4), 318–334.

Dale-Nagle, E.A., et al., 2010. Spinal plasticity following intermittent hypoxia: implications for spinal injury. Ann. N. Y. Acad. Sci. 1198, 252–259.

Dingledine, R., et al., 1999. The glutamate receptor ion channels. Pharmacol. Rev. 51 (1), 7–61.

Dougherty, B.J., et al., 2012. Contribution of the spontaneous crossed-phrenic phenomenon to inspiratory tidal volume in spontaneously breathing rats. J. Appl. Physiol. (1985) 112 (1), 96–105.

Evans, R.C., et al., 2012. The effects of NMDA subunit composition on calcium influx and spike timing-dependent plasticity in striatal medium spiny neurons. PLoS Comput. Biol. 8 (4), e1002493.

Fehlings, M.G., Tator, C.H., 1995. The relationships among the severity of spinal cord injury, residual neurological function, axon counts, and counts of retrogradely labeled neurons after experimental spinal cord injury. Exp. Neurol. 132 (2), 220–228.

Fisher, M.A., 1992. AAEM Minimonograph #13: H reflexes and F waves: physiology and clinical indications. Muscle Nerve 15 (11), 1223–1233.

Frizzo, M.E., et al., 2004. Riluzole enhances glutamate uptake in rat astrocyte cultures. Cell. Mol. Neurobiol. 24 (1), 123–128.

Fuller, D.D., et al., 2009. Graded unilateral cervical spinal cord injury and respiratory motor recovery. Respir. Physiol. Neurobiol. 165 (2–3), 245–253.

Golder, F.J., et al., 2003. Respiratory motor recovery after unilateral spinal cord injury: eliminating crossed phrenic activity decreases tidal volume and increases contralateral respiratory motor output. J. Neurosci. 23 (6), 2494–2501.

Gomperts, S.N., et al., 1998. Postsynaptically silent synapses in single neuron cultures. Neuron 21 (6), 1443–1451.

Gomperts, S.N., et al., 2000. Distinct roles for ionotropic and metabotropic glutamate receptors in the maturation of excitatory synapses. J. Neurosci. 20 (6), 2229–2237.

Goshgarian, H.G., 2003. Plasticity in respiratory motor control — invited review: the crossed phrenic phenomenon: a model for plasticity in the respiratory pathways following spinal cord injury. J. Appl. Physiol. 94 (2), 795–810.

Grooms, S.Y., et al., 2006. Activity bidirectionally regulates AMPA receptor mRNA abundance in dendrites of hippocampal neurons. J. Neurosci. 26 (32), 8339–8351.

Grossman, S.D., et al., 1999. Alterations in AMPA receptor subunit expression after experimental spinal cord contusion injury. J. Neurosci. 19 (14), 5711–5720.

Grossman, S.D., et al., 2000. Changes in NMDA receptor subunit expression in response to contusive spinal cord injury. J. Neurochem. 75 (1), 174–184.

Grossman, R.G., et al., 2014. A prospective, multicenter, phase I matched-comparison group trial of safety, pharmacokinetics, and preliminary efficacy of riluzole in patients with traumatic spinal cord injury. J. Neurotrauma 31 (3), 239–255.

Heurteaux, C., et al., 1994. Glutamate-induced overexpression of NMDA receptor messenger RNAs and protein triggered by activation of AMPA/kainate receptors in rat hippocampus following forebrain ischemia. Brain Res. 659 (1–2), 67–74.

Iwasaki, M., et al., 2014. Synergistic effects of self-assembling peptide and neural stem/progenitor cells to promote tissue repair and forelimb functional recovery in cervical spinal cord injury. Biomaterials 35 (9), 2617–2629.

Kajana, S., Goshgarian, H.G., 2008. Administration of phosphodiesterase inhibitors and an adenosine A1 receptor antagonist induces phrenic nerve recovery in high cervical spinal cord injured rats. Exp. Neurol. 210 (2), 671–680.

Karadimas, S.K., et al., 2013. A novel experimental model of cervical spondylotic myelopathy (CSM) to facilitate translational research. Neurobiol. Dis. 54, 43–58.

Kelley, A., et al., 2003. Spirometry testing standards in spinal cord injury. Chest 123 (3), 725–730.

Kerschensteiner, M., et al., 2004. Remodeling of axonal connections contributes to recovery in an animal model of multiple sclerosis. J. Exp. Med. 200 (8), 1027–1038.

Kim, J.E., et al., 2007. Anti-glutamatergic effect of riluzole: comparison with valproic acid. Neuroscience 147 (1), 136–145.

Kniest, A., et al., 2001. The glutamate antagonist riluzole and its effects upon basal and stress-induced activity of the human hypothalamus–pituitary–adrenocortical system in elderly subjects. Neuropsychobiology 43 (2), 91–95.

Lane, M.A., et al., 2008. Respiratory neuroplasticity and cervical spinal cord injury: translational perspectives. Trends Neurosci. 31 (10), 538–547.

Lang-Lazdunski, L., et al., 2000. Prevention of ischemic spinal cord injury: comparative effects of magnesium sulfate and riluzole. J. Vasc. Surg. 32 (1), 179–189.

Lee, H.K., et al., 2000. Regulation of distinct AMPA receptor phosphorylation sites during bidirectional synaptic plasticity. Nature 405 (6789), 955–959.

Li, K., et al., 2014. Overexpression of the astrocyte glutamate transporter GLT1 exacerbates phrenic motor neuron degeneration, diaphragm compromise, and forelimb motor dysfunction following cervical contusion spinal cord injury. J. Neurosci. 34 (22), 7622–7638.

Ling, L., et al., 2001. Chronic intermittent hypoxia elicits serotonin-dependent plasticity in the central neural control of breathing. J. Neurosci. 21 (5), 5381–5388.

MacFarlane, P.M., Vinit, S., Mitchell, G.S., 2011. Serotonin 2A and 2B receptor-induced phrenic motor facilitation: differential requirement for spinal NADPH oxidase activity. Neuroscience 178, 45–55.

Malenka, R.C., 2003. Synaptic plasticity and AMPA receptor trafficking. Ann. N. Y. Acad. Sci. 1003, 1–11.

Malinow, R., Malenka, R.C., 2002. AMPA receptor trafficking and synaptic plasticity. Annu. Rev. Neurosci. 25, 103–126.

Mantilla, C.B., et al., 2012. Phrenic motoneuron expression of serotonergic and glutamatergic receptors following upper cervical spinal cord injury. Exp. Neurol. 234 (1), 191–199.

Mantilla, C.B., et al., 2013. Motoneuron BDNF/TrkB signaling enhances functional recovery after cervical spinal cord injury. Exp. Neurol. 247, 101–109.

Mazzone, G.L., Nistri, A., 2011. Delayed neuroprotection by riluzole against excitotoxic damage evoked by kainate on rat organotypic spinal cord cultures. Neuroscience 190, 318–327.

McAdoo, D.J., et al., 2005. The effect of glutamate receptor blockers on glutamate release following spinal cord injury. Lack of evidence for an ongoing feedback cascade of damage → glutamate release → damage → glutamate release → etc. Brain Res. 1038 (1), 92–99.

Milanov, I.G., 1992. A comparison of methods to assess the excitability of lower motoneurones. Can. J. Neurol. Sci. 19 (1), 64–68.

Mitsushima, D., et al., 2011. Contextual learning requires synaptic AMPA receptor delivery in the hippocampus. Proc. Natl. Acad. Sci. U. S. A. 108 (30), 12503–12508.

Moon, E.S., et al., 2014. Riluzole attenuates neuropathic pain and enhances functional recovery in a rodent model of cervical spondylotic myelopathy. Neurobiol. Dis. 62, 394–406.

Mu, X., Azbill, R.D., Springer, J.E., 2000. Riluzole improves measures of oxidative stress following traumatic spinal cord injury. Brain Res. 870 (1–2), 66–72.

Myers, S.J., Dingledine, R., Borges, K., 1999. Genetic regulation of glutamate receptor ion channels. Annu. Rev. Pharmacol. Toxicol. 39, 221–241.

Nantwi, K.D., Goshgarian, H.G., 2001. Alkylxanthine-induced recovery of respiratory function following cervical spinal cord injury in adult rats. Exp. Neurol. 168 (1), 123–134.

Nicoll, R.A., Malenka, R.C., 1999. Expression mechanisms underlying NMDA receptor-dependent long-term potentiation. Ann. N. Y. Acad. Sci. 868, 515–525.

Panter, S.S., Yum, S.W., Faden, A.I., 1990. Alteration in extracellular amino acids after traumatic spinal cord injury. Ann. Neurol. 27 (1), 96–99.

Pereira, A.C., et al., 2014. Glutamatergic regulation prevents hippocampal-dependent age-related cognitive decline through dendritic spine clustering. Proc. Natl. Acad. Sci. U. S. A. 111 (52), 18733–18738.

Raineteau, O., et al., 2002. Reorganization of descending motor tracts in the rat spinal cord. Eur. J. Neurosci. 16 (9), 1761–1771.

Schwartz, G., Fehlings, M.G., 2001. Evaluation of the neuroprotective effects of sodium channel blockers after spinal cord injury: improved behavioral and neuroanatomical recovery with riluzole. J. Neurosurg. 94 (2 Suppl.), 245–256.

Schwartz, G., Fehlings, M.G., 2002. Secondary injury mechanisms of spinal cord trauma: a novel therapeutic approach for the management of secondary pathophysiology with the sodium channel blocker riluzole. In: McKerracher, L., Doucet, G., Rossignol, S. (Eds.), Progress in Brain Research. Elsevier Science B.V., pp. 177–190.

Shao, X.M., Ge, Q., Feldman, J.L., 2003. Modulation of AMPA receptors by cAMP-dependent protein kinase in preBotzinger complex inspiratory neurons regulates respiratory rhythm in the rat. J. Physiol. 547 (Pt 2), 543–553.

Shapiro, S., 1997. Neurotransmission by neurons that use serotonin, noradrenaline, glutamate, glycine, and gamma-aminobutyric acid in the normal and injured spinal cord. Neurosurgery 40 (1), 168–176 (discussion 177).

Sim, S., et al., 2013. Increased cell-intrinsic excitability induces synaptic changes in new neurons in the adult dentate gyrus that require Npas4. J. Neurosci. 33 (18), 7928–7940.

Stutzmann, J.M., et al., 1996. The effect of riluzole on post-traumatic spinal cord injury in the rat. Neuroreport 7 (2), 387–392.

Wilson, J.R., Fehlings, M.G., 2014. Riluzole for acute traumatic spinal cord injury: a promising neuroprotective treatment strategy. World Neurosurg. 81 (5–6), 825–829.

Wilson, J.R., Forgione, N., Fehlings, M.G., 2013. Emerging therapies for acute traumatic spinal cord injury. CMAJ 185 (6), 485–492.

Wu, Y., et al., 2013. Delayed post-injury administration of riluzole is neuroprotective in a preclinical rodent model of cervical spinal cord injury. J. Neurotrauma 30 (6), 441–452.

Wu, Y., Satkunendrarajah, K., Fehlings, M.G., 2014. Riluzole improves outcome following ischemia–reperfusion injury to the spinal cord by preventing delayed paraplegia. Neuroscience 265, 302–312.

Xu, G.Y., et al., 2004. Concentrations of glutamate released following spinal cord injury kill oligodendrocytes in the spinal cord. Exp. Neurol. 187 (2), 329–336.

Xu, G.Y., et al., 2008. Glutamate-induced losses of oligodendrocytes and neurons and activation of caspase-3 in the rat spinal cord. Neuroscience 153 (4), 1034–1047.

Zimmer, M.B., Goshgarian, H.G., 2005. Spontaneous crossed phrenic activity in the neonatal respiratory network. Exp. Neurol. 194 (2), 530–540.